Analysis of Dynamic Transients of High Voltage Silicon and 4H-SiC NPN BJTs

Chengjun Shen[1], Saeed Jahdi[1], Phil Mellor[1], Xibo Yuan[1], Olayiwola Alatise[2], Jose Ortiz-Gonzalez[2]

[1] University of Bristol, United Kindgom
[2] University of Warwick, United Kindgom

Corresponding author: Chengjun Shen, chengjun.shen@bristol.ac.uk

Abstract

4H-SiC vertical NPN BJTs are attractive power devices with potentials to be used as high power switching devices with high voltage ratings in range of 1.7 kV. Compared with silicon power BJTs, they particularly benefit from a large current gain to a factor of ten times higher than silicon counterparts which improves the efficiency of the gate driver. In this paper, the advantages of the 4H-SiC NPN BJTs in terms of switching transients over their silicon counterparts is illustrated by means of extensive experimental measurements and modelling. High level injection, as a common phenomenon among bipolar devices, determines the switching Speed between on-state and off-state. The two device types have been tested at 800 V with maximum temperature of 175°C and maximum collector current of 8 A. The turn-on and turn-off transition in Silicon BJT is seen to be much slower than that of the SiC BJT while the switching time will increase with increasing temperature and decreases with larger collector currents.

1 Introduction

Silicon Bipolar junction transistors (BJTs) has been used for half of the century. The low DC gain (β) in vertical Si BJTs makes it a not promising choice for applications in power electronics because complicated base drivers are needed for high base current. However, semi-insulating 4H-SiC BJTs can compete with power MOSFETs and other Substitutions of Si BJT, which have higher current density and gain [1].

In addition, BJTs have low on-state resistance due to the conductivity modulation for bipolar devices, while the gate channel used for current flow in the MOSEFT has serious ruggedness issues at high temperature application [2][3][4]. Despite thyristors are not suitable in the circuit control system, GTO thyristors made by SiC can also provide high operating temperatures, fast turn-off transients [5], etc. Furthermore, SiC BJTs have higher transconductance than SiC JFETs [2].

Thanks to the lower carrier lifetime, lower carrier mobility and much smaller width of the base & drift region, SiC BJT is predicted to have faster-switching transients [4]. At a low doped base region, especially the base and drift region of power BJT, the injected electron concentration is much higher than the base doping concentration when the high-density current injected from the collector side. This is referred to as high-level injection (HLI) in the base area. BJT undergoes large concentration of both electron and hole, which is also known as the conductivity modulation of the base region. It dramatically reduces the base resistance to allow a larger on-state current density and a lower on- state voltage drop, whereas the DC current gain and the switching characteristic are compromised [6][7]. For the dynamic transition, the variation of temperature and collector current play an important role. The dynamic switching transition can be divided into the turn-on transition and the turn-off transition which are determined by the temperature-dependent diffusion coefficient and carrier lifetime, while these two are also affected by the current level.

This paper demonstrates the performances of 4H-SiC BJTs in contrast to silicon BJTs, with analysis of Switching transients in a wide range of temperatures (25°C to 175°C) and collector current

(1 A to 8 A). Section 2 presents the theoretical models required to understand the switching transients of power BJTs while the experimental set-ups are shown in section 3. Section 4 compares experimental results with simulations following with the conclusion in Section 5.

2 Modelling Analysis

For both the Si and SiC BJT, the doping concentration of the base and drift region is much smaller than other regions in order to improve the injection efficiency from the emitter. Carrier mobility for holes (μ_p) and electrons (μ_n) in Silicon reduces with temperature [8], as:

$$\mu_n(Si) = 1360\left(\frac{T}{300}\right)^{-2.42} \quad (1)$$

$$\mu_p(Si) = 495\left(\frac{T}{300}\right)^{-2.20} \quad (2)$$

And for SiC this is:

$$\mu_n(Si) = 1140\left(\frac{T}{300}\right)^{-2.70} \quad (3)$$

$$\mu_p(Si) = 120\left(\frac{T}{300}\right)^{-3.4} \quad (4)$$

While the temperature dependence for the Diffusion coefficient can also be derived through the Einstein's equation [8]. Diffusion coefficient (D) has strong inverse temperature dependence because the temperature dependence of the of mobility is dominant, which can be determined as [8]:

$$D_n(Si) \propto \frac{1}{T^{1.42}} \quad D_n(SiC) \propto \frac{1}{T^{1.70}} \quad (5)$$

$$D_p(Si) \propto \frac{1}{T^{1.20}} \quad D_p(SiC) \propto \frac{1}{T^{2.40}} \quad (6)$$

The minority carrier lifetime under the same temperature range can be expressed as [9]–[11]:

$$\tau_n(Si) \propto T^{2.20} \quad \tau_n(SiC) \propto T^{1.72} \quad (7)$$

$$\tau_p(Si) \propto T^{2.80} \quad \tau_p(SiC) \propto T^{2} \quad (8)$$

At large currents, the injected minority carrier exceeds the doping concentration of base region causing the surge of both carriers with respect to the charge neutrality $n = p$, the mobility of both carriers decreases because of the amplified mutual Columbic interaction [8]. Assuming that the concentration of electrons is equal to the concentration of holes, the current dependencies for the carrier mobility of both carriers in Si and 4H-SiC can be defined [8] as:

$$\mu_n(Si)\&D_n(Si) \propto n^{0.91} \quad (9)$$

$$\mu_p(Si)\&D_p(Si) \propto n^{0.76} \quad (10)$$

$$\mu_n(SiC)\&D_n(SiC) \propto n^{0.61} \quad (11)$$

$$\mu_p(SiC)\&D_p(SiC) \propto n^{0.65} \quad (12)$$

and the current dependence of diffusion coefficient is the same. The total carrier lifetime τ_{tot} can also be derived as [8]:

$$\frac{1}{\tau_{tot}} = \frac{1}{\tau_{SRH}} + \frac{1}{\tau_A} \quad (13)$$

where τ_{SRH} and τ_A are the carrier lifetime from the Shockley-Read-Hall recombination and Auger recombination process. The effect of τ_A is negligible at low collector current, therefore the total lifetime increases with rising collector current as determined purely by the τ_{SRH}. For the high injection level, the Auger lifetime plays a more important role which increases with larger collector currents, leading to the increase of total lifetime. In SiC, the electrically active defects arising in the substrate increases the τ_{SRH} leading to the lower lifetime compared with that of Si [12].

2.1 Turn-ON transient

The carrier setup phase, the current increase phase and voltage drop phase are included in the turn-ON transition. First, enough charge must be built up in the base and drift region to turn-ON the BJT as 'transient time', given by:

$$t_{transient} = \frac{W_B^2}{2D_n} \quad (14)$$

Where the W_B is the width of the base region. After the storage phase, enough minority carrier charge in the base region Q_{nB} promotes the current flow. The rise of collector current during this period in relation to the carrier concentration can be expressed as:

$$J_C = \frac{qD_n d_n}{d_x} = \frac{qD_n n_B}{W_B} = \frac{2D_n \beta J_B t_{I-on}}{W_B^2} \quad (15)$$

Consequently, the current rise time t_{Ion} is given as:

$$t_{I-on} = \frac{W_B^2 J_C}{2D_n \beta J_B} = \frac{W_B^2}{2D_n} \quad (16)$$

The D_n reduces with increasing temperature, leading to the increase in switching time, and further increased in higher collector currents. Afterwards, the collector voltage drops to the steady-state level. This period is defined as the ratio of the stored minority carrier charge at the base-collector junction (Q_{sc}) to the collector current as:

$$t_{V-on} = \frac{Q_{SC}}{J_C} = \frac{qW_B N_B + qW_D N_D}{J_C} \quad (17)$$

The voltage level in this phase is limited by the stored charge in the drift region, i.e. The depleted part of the drift region become smaller which lead to a smaller voltage level. Faster voltage transition is expected at high collector current. However, the smaller J_C is predicted in high temperatures because the diffusion coefficient decreases with temperature.

At turn-off, a reverse base current (J_{BR}) is applied to extract the stored carrier from the base and drift regions. This time is known as the storage time or delay time, namely:

$$Q_{nB}(t) + Q_{SC}(t) = J_{BR} \cdot t_S \quad (18)$$

And the storage time t_S is given by:

$$t_S = \frac{J_C}{J_{BR}} \left(\frac{W_{NM}^2}{4D_n} \frac{J_C D_P}{J_C D_P + J_{BR} D_n} + \frac{W_B^2}{2D_n} \right) \quad (19)$$

where

$$W_{NM} = \frac{2qD_n}{J_c} \left(P_{NS}(0) - N_D \right) \quad (20)$$

At this stage the voltage rise time is shown in Eq.21 and the current drop-time is decided by the remaining carriers after the turn-off of the collector voltage, as given in Eq.22, with the diffusion length L_n expressed in Eq.23.

$$t_{V-off} = \frac{\sqrt{2\varepsilon q N_D V_C}}{2\frac{p(W_S)}{W_S} q D_p} \quad (21)$$

$$t_{I-off} = \frac{W_E - X_V}{\frac{2W_E D_n}{\beta W_B^2} - \frac{D_n}{L_n}} \quad (22)$$

$$L_n = \sqrt{\tau_n D_n} \quad (23)$$

From the equation 23, the temperature dependence of the diffusion length is decided by the trade-off between D_n and τ_n while the temperature dependence of both are shown in the equation 1-4 and equation 7-8. As the result, the diffusion length is almost temperature independent due to the opposite change rate between D_n and τ_n. Nevertheless, the slower current drop is caused by the temperature dependent D_n. Under high current levels, the t_{I-off} is increased as the decrease in D_n is more dominant compared to the decrease of L_n.

3 Experimental Set-Up

A wide range of experimental measurements and simulations are done to observe the effect of collector's high current injection and temperature on the latest high voltage silicon and 4H-SiC power BJTs. High voltage BJTs are mounted on a double-pulse test board with a specific base driver used for switching, their parameters are specified in Table.1 and Table.2 separately. A 1.2 kV SiC Schottky barrier diode and a 4 mH load inductor are also connected to the device under test (DUT).The base resistance of the gate driver is changed from 3.75 to 7 Ω while temperature is increased from 25°C to 175°C in 25°C increments. The collector current is controlled by the charging pulse length t_{Q1}, increased linearly from 5 μs to 40 μs in steps of 5 μs while every 5 μs roughly equals to an increase of 1 A in collector current.

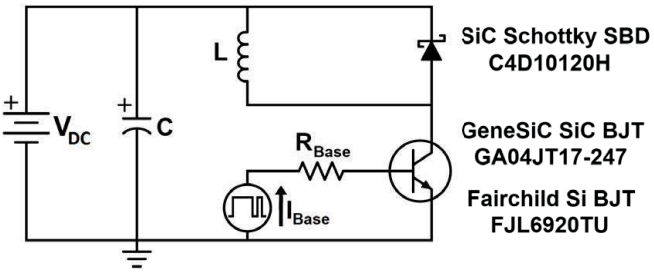

Fig. 1: The circuit diagram of the double-pulse test

The test board has a 5 mF DC link capacitor bank to stabilize the voltage V_{DC}. The power BJTs are the Fairchild silicon BJT and GeneSiC 4H-SiC BJT, while the high-side freewheeling diode is a CREE SiC Schottky diode. The voltage applied to both the silicon and SiC BJT is 800 volts. Although there is still a gap between the blocking voltages, they are selected carefully after exploring many available devices to choose the closest possible ratings for the tests in terms of voltage & current. Two GW-Instek GDP-100 100 MHz voltage probes and a Tektronix TCP312A 100 MHz current probe are used to obtain waveforms of measurement. A

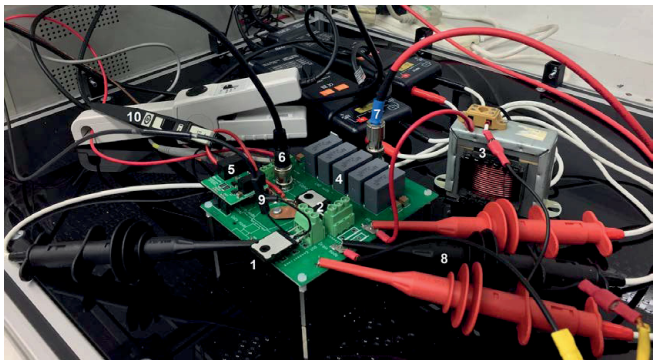

Fig. 2: Components on the test board GA100SBJT12-FR4 includes:1- BJT transistor, 2- Schottky Diode, 3- Load Inductor, 4- DC Capacitors, 5-GA03IDDJT30-FR4 Base Driver, 6- Input Signal, 7- HV power supply, 8-Voltage Probes, 9-Rogowski Coil and 10- Current Probe

100 nF de-coupling capacitor is connected between the cathode of the Schottky Barrier Diode (SBD) and the emitter side of the BJT closest to the DUTs. Agilent 33220A 20 MHz arbitrary waveform generator is used for adjusting the t_{Q1}. Stray inductance of 60 nH is due to the inevitable distance among the components. A similar circuit model is designed in LTSpice to model switching transients to confirm the experimental results. The DC current gain of SiC BJT, as shwon in Table.3, is much higher than its Silicon counterpart [8]. The drift and base doping concentration of SiC device are higher than that of the Silicon BJT, enabling SiC BJT to be less influenced by the injection level [8]. The power dissipation of the SiC device is lower though due to its smaller dimensions.

Tab. 1: Parameters of GA100SBJT12-FR4 Board Components.

Parameter	Symbol	Value
C_{DC}	DC Capacitor	5 mF
C_{HF}	De-Coupling Capacitor	100 nF
L	Load Inductor	4 mH
V	Test Voltage	800 V
I	Test Current	1-8 A
t_{Q1}	Charging Pulse Length	5-40 μs
t_{Q2}	Switching Pulse Length	8 μs
t_{Qnil}	Gap between Pulses	30 μs
T	Temperature Range	25-175℃
R_{Base}	Base Resistance Range	0-3.3 Ω
L_{Stray}	Estimated Parasitic Inductance	60 nH

Tab. 2: BJT Base Driver GA03IDDJT30-FR4 Parameters.

Symbol	Parameter	Value
V_{CC}	Driver Input Supply Voltage	12 V
$I_{B,switch}$	Output Peak Base Current	4 A
$I_{B,on-state}$	Output On-state Base Current	0.35 A
t_{rise}	Output Base Voltage Rise Time	21 ns
t_{fall}	Output Base Voltage Fall Time	14 ns
C_B	Base Capacitor	10 nF
R_{B1}	Charging Resistor	1 kΩ
R_{B2}	Base Resistance	3.75 Ω

Tab. 3: Power Silicon and 4H-SIC NPN BJT as DUTs T= 25°C.

	4H-SiC	Si
Model	GA04JT17-247	FJL6920
Manufacturer	GeneSiC	Fairchild/ON
Collector-Emitter Voltage (V)	1700	800
Collector Current (A)	15	20
Collector Current above 150℃ (A)	5	20
Power Dissipation (W)	106	200
DC Current Gain - β (-)	100	8
J-C Thermal Resistance (℃/W)	1.41	0.625
B-E Saturation Voltage (V)	3.45	1.5

4 Experimental Results

Fig. 3 & Fig. 4 shows the double-pulse test results in two different temperatures with base resistance of 3.5 Ω and 7 Ω at 800 V. Fig. 3(a) shows a period of delay between the base turn-off and the collector current drop in silicon BJT, which increases with rise of temperature. The diffusion coefficient D_n is inversely proportional to temperature, leading to an increase of storage time. The base current is constant during the increase of collector current since it operates at the saturation region. In Fig. 3(b), both the base and collector current are turned on and off almost instantaneously for the 4H-SiC BJT, due to the much lower carrier lifetime and the significantly smaller dimensions enabling the decrease of the storage and transient time. The rating current of SiC device, as shown in Table.3, is found to decrease at high temperatures. Fig. 3(b) shows this issue during the HIL which reduces the current level in the second pulse, leading to a ”notch” in the waveform. This problem will get worse at high base resistance since the second pulse is almost erased, as seen in Fig. 3(c).

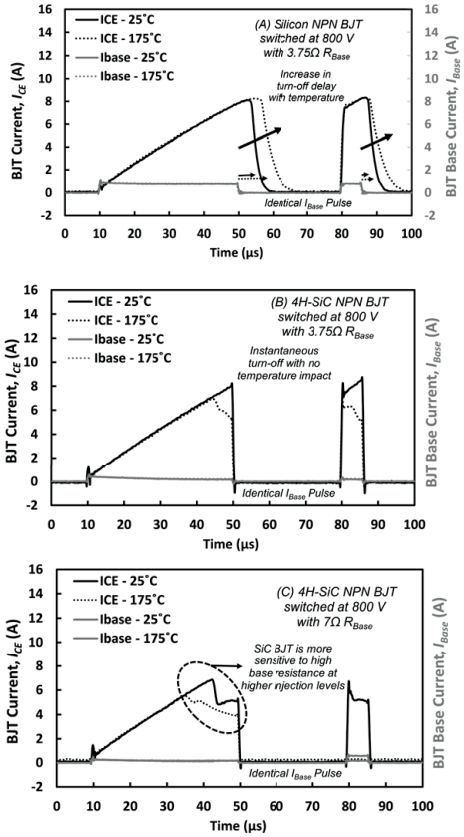

Fig. 3: Double pulse test results of the collector and base current for (a) Silicon BJT with the R_{base} of 3.75 Ω and (b) 4H-SiC NPN BJT with the R_{base} of 3.75 and (c) 7Ω indicating the temperature-dependent delay under the same base current.

Fig. 4 shows the double-pulse test result with respect to different collector currents at 800V when T=175℃. The collector current applied in this case is 1 A and 8 A separately (derived by estimation, the actual current level will vary due to the delay), while all other parameters are the same. The average delay time is 15μs for the Silicon BJT which deteriorates its performance, especially at high frequency as extra power losses are caused by the prolonged collector current. With the larger collector current, the delay time is reduced due to the smaller W_{NM}. Meanwhile, the much lower delay time in SiC BJT in Fig. 4(b) is expected by its dimensions. The high temperature instability is also observed, i.e. the current at first pulse decreased to a lower level since the collector current of 8 A delivers the high-injection at 150℃. During the measurements, the SiC BJT does not function properly at 175℃ since it failed at 150℃. The Silicon BJT, on the other hand, worked well until the collector current exceeding 7 A at 175℃. Therefore, during stressed measurements and due to the risk of damage to the device in high temperatures and currents, the temperature of up to 150℃ and collector current of up to 7 A are applied to avoid further failure. The

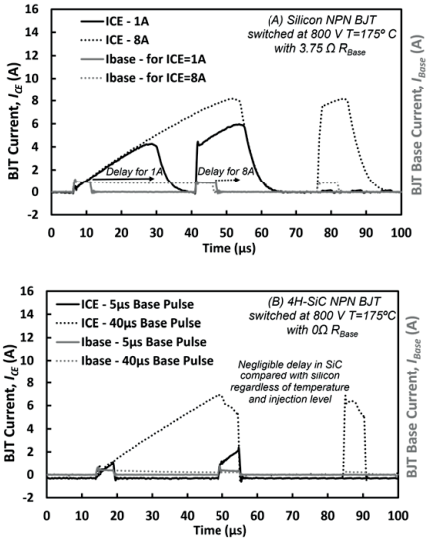

Fig. 4: The double pulse test results regarding the collector and base current at 150℃ for (a) Silicon and (b) 4H-SiC BJT, with R_{base} of 3.75 Ω to analyze the turn-off delay with respect to different collector currents under the same base current.

collector current at turn-on and turn-off transients are shown in Fig. 5 and Fig. 6 for both Silicon and SiC BJT. The turn-off delay is previously shown to get worse at elevated temperatures, which will in turn increase the collector current increase as the temperatures rises as effectively the length of the first pulse increases. Meanwhile, the value of delay decreases with increased collector currents.

When comparing Fig. 5(a) and Fig. 5(b), the much smaller W_B plays a significant role to reduce the t_{lon} for the SiC BJT, while the increase of turn-on period is expected by the decreasing the diffusion coefficient at high temperatures. Looking at the different trends of Silicon and SiC devices in Fig. 5(a) and Fig. 5(b), the much smaller W_B can be seen to play a significant role to reduce the t_{lon} for the SiC BJT, while with increase of temperature as shown in Fig. 5(b), the turn-off transient is slower. This is because of the increased carrier lifetime, and the lower diffusion coefficient which leads to a larger t_{I-off}, whereas the t_{I-off} is always lower for the SiC device because of the much lower carrier lifetime and the smaller dimensions of the

die. Further measurements have indicated that as the collector current increases with the pulse width, the turn-off time further increases because of the decrease of diffusion coefficient, and the increase in carrier lifetime at high currents. Although the diffusion coefficient of SiC is less dependent on the collector current, this is hard to observe since the value of t_{I-off} is largely influenced by the square of W_B as shown previously.

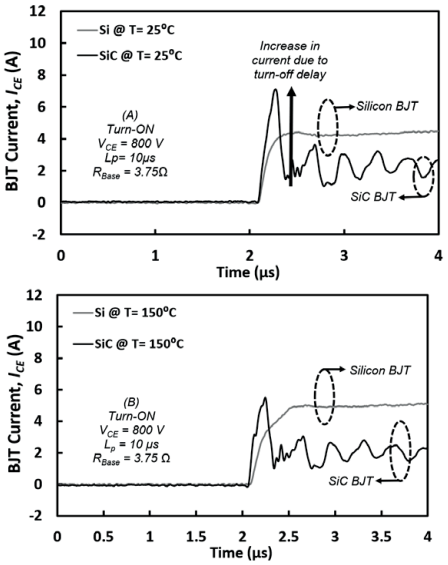

Fig. 5: Turn-on transient of silicon and 4H-SiC BJT with pulse length of 10μs with at (a) 25℃ and (b) 150℃ for the BJT collector current.

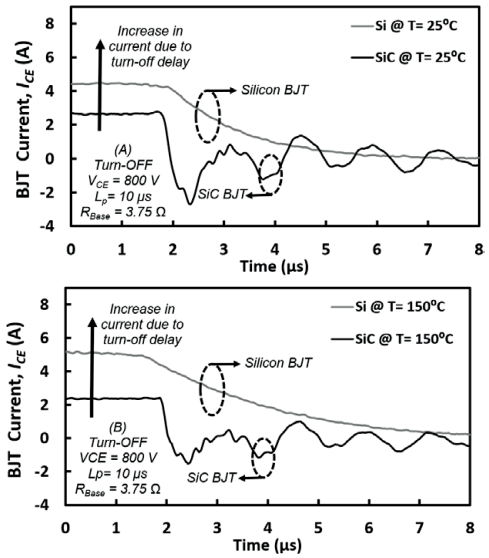

Fig. 6: Turn-off transient of silicon and 4H-SiC BJT with pulse length of 10μs with at (a) 25℃ and (b) 150℃ for the BJT collector current.

The results of Fig. 5 and Fig. 6 match well with results of the simulations in Fig. 7. Although there is some error is modeling of the oscillations by the LTSpice, the *dI/dt* is found to be a good match in the model.

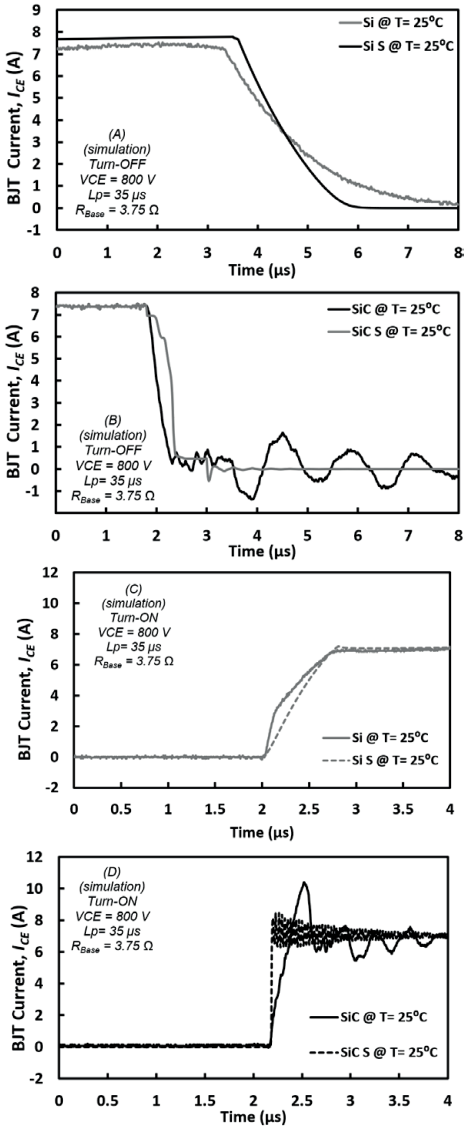

Fig. 7: The simulation results for the measurements shown in Fig. 5 & Fig. 6 for (a) Si BJT at turn-off and for (b) SiC BJT at turn-off for (c) Si BJT at turn-on and for (D) SiC BJT at turn-on, to analyze the validity of the models.

The SiC device has faster voltage transients in Fig. 8 and Fig. 9 as was predicted previously in the modeling section. At turn-on transients in Fig. 8, the temperature-dependent diffusion coefficient decreases the J_C leading to the larger t_{von} (refer to description provided in Section 2), resulting in the slower transient in Fig. 8(b). The higher collector current can directly reduce the t_{von} in high injection

level. At turn-off transients shown in Fig. 9(a) & (b), the voltage turn-off process is slower at high temperatures because of the temperature-dependent diffusion coefficient which increases the value of $t_{v\text{-}off}$. The slower performance is also due to the current dependent D_p which also increases $t_{v\text{-}off}$. Furthermore, the stored charge Q_{nB} and Q_{SC} are inversely proportionate to the diffusion coefficient, leading to more charge stored in the drift & base region, which reduces the depletion region, resulting in a smaller voltage drop at high current & temperature. The Q_{nB} and Q_{SC} built at the turn-on is the same as that removed at turn-off, therefore the same temperature- and current-dependence can be seen in these figures.

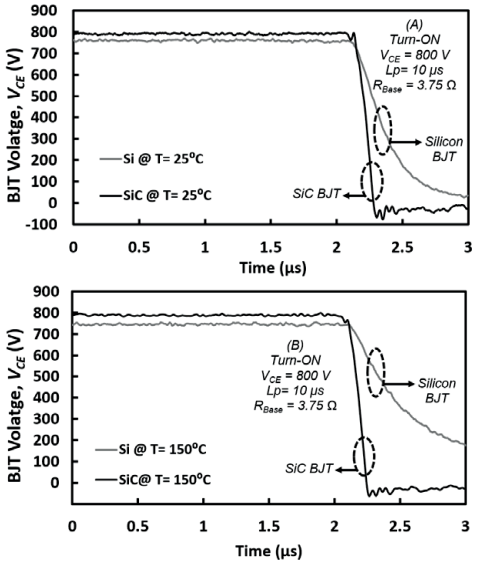

Fig. 8: Turn-on transient of silicon and 4H-SiC BJT with pulse lengths of 10μs at (a) 25℃ and (b) 150℃ for BJT collector voltage.

Tab. 4: Measurements of transient delays of the Silicon & 4H-SiC NPN BJT at turn-on & turn-off.

	Turn-ON		Turn-OFF	
	Si	SiC	Si	SiC
Q at 2 A	0.4 μs	0.06 μs	12 μs	1.2 μs
Q at 8 A	0.44 μs	0.05 μs	4.3 μs	0.09 μs
t_I at 2 A	0.405 μs	0.132 μs	4.8 μs	0.104 μs
t_I at 8 A	0.415 μs	0.130 μs	5.12 μs	0.106 μs
t_V at 2 A	1.97 μs	0.3 μs	3.6 μs	0.7 μs
t_V at 8 A	1.38 μs	0.28 μs	4.0 μs	0.75 μs

The time taken to turn-on and turn-off are shown in the Table. 4 for both the Si and SiC NPN BJTs. At the turn-on transient, the $t_{transient}$ of the Silicon BJT

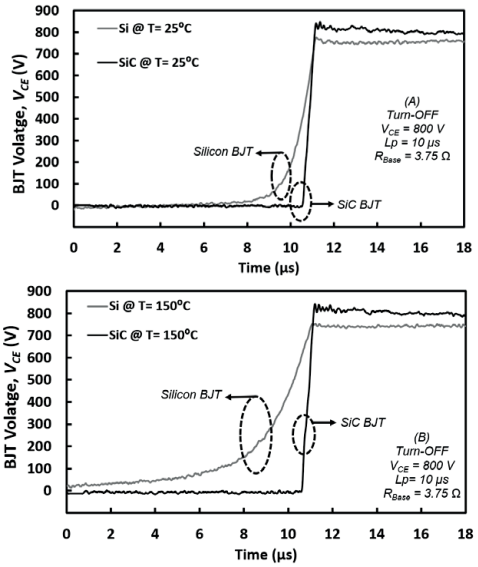

Fig. 9: Turn-off transient of silicon and 4H-SiC BJT with pulse lengths of 10μs at (a) 25℃ and (b) 150℃ for BJT collector voltage.

is increased with increase of the collector current as a result of the decreased D_n in high currents. The $t_{I\text{-}on}$ is also increased for the same reason. The $t_{V\text{-}on}$, on the other hand, decreases with J_C which is the most dominant component to reduce the total turn-on time at HLI. A faster turn-on for the SiC BJT is predicted due to the significantly smaller dimensions of the base and drift region. In high temperatures, the $t_{transient}$ and $t_{I\text{-}on}$ are increased because of the decrease in the diffusion coefficient, while the decreased D_n also reduces the J_C and prolonging the voltage turn-on time $t_{V\text{-}on}$. At the turn-off transient, the $t_{V\text{-}off}$ of the Silicon BJT increases as the diffusion coefficient D_p is decreased at HLI. The $t_{I\text{-}off}$ also increases because the decrease in D_n is dominant to the decrease of L_n. Nevertheless, the increase in these two terms is compensated by the reduction of t_S, as the decreased W_{NM} is more significant compared to the drop of D_n, reducing the total turn-off time at HLI. These trends hold true for the SiC BJT at turn-off, even with the much smaller width of the base (W_B) region, which contributes to a reduction of the turn-off time by an order of magnitude. It is seen that the t_S is much larger than the $t_{transient}$ since the charge depletion phase removes more carriers than those built initially. In high temperatures, the t_S and $t_{V\text{-}off}$ are increased because of the decrease in diffusion coefficient. Since the decrease of D_n is dominant, the $t_{I\text{-}off}$ are also increased.

5 Conclusion

In the full paper, the high voltage measurements of dynamic transient characteristics of silicon and 4H-SiC NPN BJTs will be presented, together with comprehensive modelling and simulation analysis. Measurements are done in a wide range of temperatures (up to 150℃) and collector current (up to 8 A). The voltage and current transient times in 4H-SiC BJT are, as demonstrated in experiment, at least 10 times shorter than that in silicon BJT because of the smaller width in the base region. The much smaller turn-off delay (t_S) can also reduce the on-state current level, minimizing both the on-state and switching power losses in SiC BJT. As for the Si BJT, the turn off time is much larger than that of turn-on phase because of the substantial value of t_S. Therefore, it is shown experimentally that Si BJTs perform more efficiently in HLI condition.

References

[1] J. Lutz **and** et al., *Semiconductor Power Device*, 2 **edition**. Springer, 2018.

[2] N. Zhang, "Silicon carbide bipolar junction transistors for high temperature sensing applications," 2016.

[3] Jianhui Zhang, Y. Luo, P. Alexandrov, L. Fursin **and** J. H. Zhao, "A high current gain 4h-sic npn power bipolar junction transistor," *IEEE Electron Device Letters*, **jourvol** 24, **number** 5, **pages** 327–329, 2003. DOI: 10.1109/LED.2003.812531.

[4] S. Jahdi, M. Hedayati, B. H. Stark **and** P. H. Mellor, "The impact of temperature and switching rate on dynamic transients of high-voltage silicon and 4h-sic npn bjts: A technology evaluation," *IEEE Transactions on Industrial Electronics*, **jourvol** 67, **number** 6, **pages** 4556–4566, 2020. DOI: 10.1109/TIE.2019.2922918.

[5] X. Xu, K. Zhou, L. Zhang, Z. Li, L. Li **andothers**, "High-voltage 4h-sic gto thyristor with multiple floating zone junction termination extension," **in***2018 1st Workshop on Wide Bandgap Power Devices and Applications in Asia (WiPDA Asia)* 2018, **pages** 149–152. DOI: 10.1109/WiPDAAsia.2018.8734630.

[6] B. Buono, R. Ghandi, M. Domeij, B. G. Malm, C. Zetterling **and** M. Östling, "Influence of emitter width and emitter–base distance on the current gain in 4h-sic power bjts," *IEEE Transactions on Electron Devices*, **jourvol** 57, **number** 10, **pages** 2664–2670, 2010. DOI: 10.1109/TED.2010.2061854.

[7] B. Buono, R. Ghandi, M. Domeij, B. G. Malm, C. Zetterling **and** M. Ostling, "Modeling and characterization of current gain versus temperature in 4h-sic power bjts," *IEEE Transactions on Electron Devices*, **jourvol** 57, **number** 3, **pages** 704–711, 2010. DOI: 10.1109/TED.2009.2039099.

[8] J. Baliga, *Fundamnetal of Power Semiconductor Device*. Springer, 2019.

[9] X Li, Y Luo, L Fursin, J. Zhao, M Pan **andothers**, "On the temperature coefficient of 4h-sic bjt current gain," *Solid-State Electronics*, **jourvol** 47, **number** 2, **pages** 233 –239, 2003. DOI: https://doi.org/10.1016/S0038-1101(02)00200-9.

[10] Y. C. Gerstenmaief, "A study on the variation of carrier lifetime with temperature in bipolar silicon devices and its influence on device operation," **in***Proceedings of the 6th International Symposium on Power Semiconductor Devices and Ics* 1994, **pages** 271–274. DOI: 10.1109/ISPSD.1994.583738.

[11] A. Udal **and** E. Velmre, "Investigation of charge carrier lifetime temperature-dependence in 4h-sic diodes," **in***Silicon Carbide and Related Materials 2006* **jourser** Materials Science Forum, **volume** 556, Trans Tech Publications Ltd, **august** 2007, **pages** 375–378. DOI: 10.4028/www.scientific.net/MSF.556-557.375.

[12] C. A. Fisher, "Development of 4h-sic pin diodes for high voltage applications," 2014.